Electric Grüneisen parameters for a biaxial spin-chain system

A. A. Zvyagin

B. I. Verkin Institute for Low Temperature Physics and Engineering of the National Academy of Sciences of Ukraine, Nauky Avenue, 47, Kharkiv 61103, Ukraine;

Max-Planck Institut für Physik komplexer Systeme, Nöthnitzer Strasse, 38, D-01187 Dresden, Germany;

and V. N. Karazin Kharkiv National University, 4, Svoboda Square, Kharkiv 61022, Ukraine

(Received 4 November 2022; accepted 26 January 2023; published 7 February 2023)

The electric Grüneisen parameter, which characterizes the electrocaloric effect in the quantum spin system, has been introduced. We have calculated the electric Grüneisen parameter for the biaxial spin-chain system with strong coupling between the spin and the electric subsystems. It is shown that the low-temperature electric field dependence of the electric Grüneisen parameter manifests features at the critical values of the electric field and tends to constant at high temperatures. It is determined by the quantum critical points of the spin system. Such a behavior of the electric Grüneisen parameter can be observed in electrocaloric experiments with spin-chain materials.

DOI: 10.1103/PhysRevB.107.054403

I. INTRODUCTION

Electrocaloric effect determines the temperature change of the system due to adiabatic application or removal of an external electric field [1–3]. Similar to the magnetocaloric effect, the electrocaloric one permits cooling or heating of the system. For the description of the caloric effect of solids and phase transitions associated with the change of the volume, the Grüneisen parameter is often used. The Grüneisen parameter (also known as the Grüneisen ratio) was first introduced for the Einstein model to study the quantitative characteristics of the effect of volume change of a crystal lattice on its vibrational frequencies [4,5]

$$\Gamma = \frac{V}{\Omega}\frac{\partial \Omega}{\partial V}, \tag{1}$$

where Ω is the frequency of phonons and V is the volume. That original Grüneisen parameter is dimensionless. It can be rewritten as $\Gamma = (V/c_V)(\partial \mathcal{S}/\partial V)$, where $\mathcal{S}$ is the entropy of the system, and c_V is the specific heat at the fixed volume.

Later, it was proposed to study the magnetic Grüneisen parameter [6,7]

$$\Gamma_m = -\frac{\frac{\partial \mathcal{S}}{\partial H}|_T}{T\frac{\partial \mathcal{S}}{\partial T}|_V} \tag{2}$$

for fixed temperature T and volume, respectively. Here H is the external magnetic field and T is the temperature. In the following, we use the units in which the effective magneton $g\mu_B = 1$, with g being the effective g factor and μ_B being the Bohr magneton, and with the Boltzmann constant $k_B = 1$, for simplicity. Notice that the magnetic Grüneisen parameter is not dimensionless.

The magnetic Grüneisen parameter describes the magnetocaloric effect; i.e., it shows the connection between the variation of the external magnetic field, which changes the population imbalance for spins and the cooling of the system. The magnetic Grüneisen parameter can be written as $\Gamma_m = \alpha_{mT}/c_V$, where α_{mT} is the magnetic expansion coefficient. The most significant changes of the magnetic Grüneisen parameter take place at the lines of phase transitions, including the quantum critical points. For example, at the quantum critical point the magnetic Grüneisen parameter changes its sign [7]. The magnetic Grüneisen parameter is often used in experiments for the quantitative description of magnetocaloric effect in many systems, including low-dimensional magnetic systems [8], heavy fermion ones [9], and quantum critical phenomena in solids [10].

Systems with strong coupling of spin, electric, and elastic subsystems attract the attention of researchers. The nature of such a coupling is as follows. Nonmagnetic ions (called ligands), which surround magnetic ions, define the crystalline electric field, which acts on magnetic ions. That field, together with the spin-orbit interaction and the exchange coupling, determines the single-ion magnetic anisotropy, or the magnetic anisotropy of the indirect exchange interaction between spins in the spin system. Strains of the elastic subsystem change the distribution of ligands, affecting the internal crystalline electric field. Similarly, the external electric field, as the crystalline electric field of ligands, acts on the orbital moments of magnetic ions. Due to the spin-orbit coupling, those electric fields and strains change the single-ion spin anisotropy and/or the anisotropy of the indirect exchange coupling between spins. The external magnetic field, in turn, changes the relative directions of spins, and, due to the spin-orbital coupling, the

Published by the American Physical Society under the terms of the Creative Commons Attribution 4.0 International license. Further distribution of this work must maintain attribution to the author(s) and the published article's title, journal citation, and DOI. Open access publication funded by the Max Planck Society.

relative directions of orbital moments of ligands, affecting their positions via strains (as in the Jahn-Teller effect). Hence, the distribution of charges is changed, affecting the electric characteristics of the system.

Those systems are interesting from pure physical grounds. In addition, they are important for modern technology from the viewpoint of applications of magneto-electro-elastic effects which can be governed by external fields and strains, in microelectronics, spintronics, optical devices, etc., as, e.g., switching devices, or writing and reading devices for memory storage. One of the most known examples of such systems are multiferroics, in which orderings can exist in some of mentioned subsystems, and they attract great attention [11–17]. For the description of such ordered magnetic and electric systems, classical electrodynamics can be used [18]. However, obviously, quantum effects can be also manifested in compounds with interacting spin, charge, and elastic subsystems. It is interesting to consider a quantum many-body spin system, in which interactions among spin, electric, and elastic subsystems can take place. Spin-chain compounds are systems in which spin-spin interactions in one direction are much stronger than in other ones. They can serve as a good testing ground for the manifestation of the interaction among electric, magnetic, and elastic subsystems. In such systems, the effective reduced dimensionality of the spins causes the enhancement of quantum and thermal fluctuations, which destroys magnetic ordering at nonzero temperatures [19]. However, the coupling between spins along the distinguished direction can be very strong, and hence those systems manifest quantum many-body effects. It is also very important that spin-1/2 chains permit exact theoretical results [20], which give the opportunity to check them in comparison with the data of experiments in spin-chain compounds. Obviously, quantum effects in spin-chain compounds manifest themselves at low temperatures, and therefore cooling such systems with the help of magnetocaloric or electrocaloric effects are very important for practical purposes.

II. ELECTRIC GRÜNEISEN PARAMETER

For magnetic systems with the magnetoelectric interaction, we can introduce by analogy with the magnetic Grüneisen parameter, the electric Grüneisen parameter

$$\Gamma_e = -\frac{\frac{\partial \mathcal{S}}{\partial E}|_T}{T\partial\mathcal{S}\partial T|_V} \equiv -\frac{\alpha_{eT}}{c_V}, \tag{3}$$

where α_{eT} is the electric expansion coefficient. The electric Grüneisen ratio shows the quantitative relation between the change of the external electric field, which also can change the population imbalance for quantum spin systems, and the refrigeration of the considered system.

In this study, we calculate the electric Grüneisen parameter for the quantum spin-1/2 chain compound with the strong magnetoelectric interaction. We show that the behavior of such a Grünesen ratio in the spin-chain system is determined by the quantum critical points, which exist there [21,22]. It is important to stress that those ground-state phase transitions manifest themselves in the behavior of electric Grüneisen parameter, the characteristic of the electrocaloric effect, at nonzero temperature.

III. THE CONSIDERED SYSTEM

The Hamiltonian of the considered biaxial (with the orthorhombic magnetic anisotropy) spin-1/2 chain system, in which the spin subsystem is coupled to the electric one, can be written as [21,22]

$$\begin{aligned}\mathcal{H} = &-\sum_n \left(J_x S_n^x S_{n+1}^x + J_y S_n^y S_{n+1}^y + J_z S_n^z S_{n+1}^z\right) \\ &+ a_1 E_y \sum_n \left(S_n^x S_{n+1}^y - S_n^y S_{n+1}^x\right) + a_2 E_y \sum_n \left(S_n^x S_{n+1}^y \right. \\ &\left. + S_n^y S_{n+1}^x\right) + a_3 E_x \sum_n \left(S_n^x S_{n+1}^x - S_n^y S_{n+1}^y\right) \\ &- H \sum_n S_n^z, \end{aligned} \tag{4}$$

where $S_n^{x,y,z}$ are the operators of spin projections of the spins-1/2 situated at the site n, H is the magnetic field H directed along the z axis, and $J_{x,y,z}$ are the parameters of the magnetically anisotropic exchange interaction. It is useful to introduce $I = (J_x + J_y)/2$ and $J = (J_x - J_y)/2$. Then, $E_{x,y}$ are the components of the external electric field and $a_{1,2,3}$ are the coefficients of the magnetoelectric coupling (for the y direction of the electric field they are related to the exchange-antisymmetric and exchange-symmetric couplings). The form of the electromagnetic coupling in the Hamiltonian is the particular case of the general interactions between spin and electric degrees of freedom $\sum_{m,n}\sum_{ipq} a_{ipq} E_i S_n^p S_m^q$, where n, m numerate the lattice sites, and $i, p, q = x, y, z$ [18] with $a_{1,2,3}$ being the components of the tensor a_{ipq}. Notice that we use the form of magnetoelectric coupling similar to Ref. [23], where the studied effects were observed in the magnetically ordered multiferroic.

First, one can see that the electric field, directed along the x axis, renormalizes the exchange parameter $J \to (J - a_3 E_x)$. Let us then consider the effect of E_y. Suppose that for the spin chain the open boundary conditions are imposed. Then, using the rotation of all spins with respect to the axis z by the angle ψ, we can rewrite the Hamiltonian (4) as

$$\begin{aligned}\mathcal{H} = &-I \sum_n \left(S_n^x S_{n+1}^x + S_n^y S_{n+1}^y\right) \\ &- J_1 \sum_n \left(S_n^x S_{n+1}^x - S_n^y S_{n+1}^y\right) - J_z \sum_n S_n^z S_{n+1}^z \\ &- H \sum_n S_n^z + a_1 E \sum_n \left(S_n^x S_{n+1}^y - S_n^y S_{n+1}^x\right), \end{aligned} \tag{5}$$

where $J_1 = [(J - a_3 E_x)^2 + (a_2 E_y)^2]^{1/2}$ and $\tan 2\psi = -(a_2 E_y)/(J - a_3 E_x)$. The angle ψ does not enter the expression for the Hamiltonian for the open chain.

Now we can obtain some analytical results for the electric Grünesen parameter as a function of the temperature and applied electric and magnetic field. We can use the Jordan-Wigner transformation [24] connecting spin operators and operators of creation and destruction of spinless fermion operators and the Fourier transformation. The Hamiltonian (5)

takes the form

$$\mathcal{H} = -\frac{NH}{2} - \frac{N\Delta}{4} + \sum_k \Big[[H - I_1 \cos(k-\phi)] a_k^\dagger a_k - \frac{J_1}{2}(a_{-k} a_k e^{-ik} + \text{H.c.}) - \frac{J_z}{N}\cos(k)\rho_{-k}\rho_k \Big], \quad (6)$$

where $a_k^\dagger$ (a_k) creates (destroys) the spinless fermion with the quasimomentum k, $I_1 = [I^2 + (a_1 E_y)^2]^{1/2}$, $\tan\phi = (a_1 E_y)/I$, and $\rho_k = \sum_p a_{p+k}^\dagger a_p$.

IV. RESULTS

Let us start our analysis with the simplest case $J_z = 0$ for which the Hamiltonian (6) is the quadratic form of Fermi operators. Using the Bogoliubov transformation, we obtain for the free energy of the system per site

$$F = -\frac{T}{N}\sum_k \ln\,[2\cosh(\varepsilon_k/2T)], \quad (7)$$

where T is the temperature, and

$$\varepsilon_k = a_1 E \sin(k) + \sqrt{[H - I\cos(k)]^2 + J_1^2 \sin^2(k)}. \quad (8)$$

Using the expression for the free energy, it is easy to calculate the specific heat per site

$$c_V = (4T^2 N)^{-1} \sum_k \frac{(\varepsilon_k)^2}{\cosh^2(\varepsilon_k/2T)}. \quad (9)$$

We can see that for the spin-chain system the specific heat decays at high temperatures as T^{-2}. At low temperatures, the specific heat is exponentially small if the spectrum (8) is gapped, and it manifests the linear growth with T if the spectrum is gapless. For intermediate temperatures, the temperature behavior of the specific heat of the spin chain manifests the maximum [20]. Such a behavior is characteristic for spin-chain systems for nonzero J_z also [20].

For the electric expansion coefficients per site, we get

$$\alpha_{exT} = (4T^2 N)^{-1} \sum_k \frac{a_3 (J - a_3 E_x)[\sin(k)]^2}{\cosh^2(\varepsilon_k/2T)},$$

$$\alpha_{eyT} = -(4T^2 N)^{-1} \sum_k \frac{\sin(k)\varepsilon_k}{\cosh^2(\varepsilon_k/2T)} \times \left[a_1 + \frac{a_2^2 \sin(k)}{\sqrt{[H - I\cos(k)]^2 + J_1^2 \sin^2(k)}} \right], \quad (10)$$

where the first expression is for the electric field E_x and the second one is for E_y. The electric expansion coefficients also decay at high temperatures as T^{-2}. Hence, the electric Grüneisen ratios tend to constant at high temperatures, similar to the magnetic Grüneisen parameter [6,7]. The low-temperature behavior of the electric expansion coefficients also depends on the features of the spectrum of elementary excitations of the system. Hence, the ground state and the low-temperature behavior of the electric Grüneisen parameters are determined by those features, too.

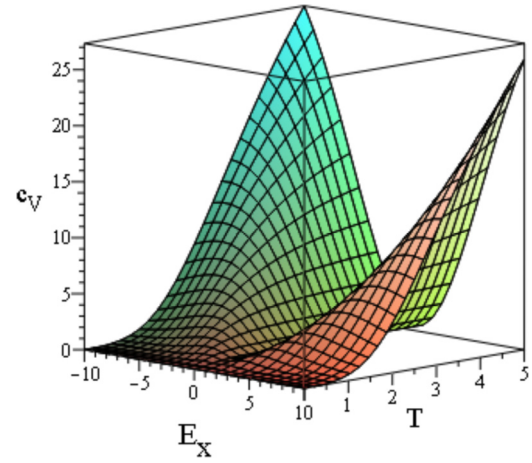

FIG. 1. The specific heat of the biaxial spin chain in the absence of external magnetic field as a function of the temperature and the applied external electric field E_x.

The low-temperature behavior of all thermodynamic characteristics of the spin chain is determined by quantum critical points (lines), governed by the magnetic field H and the electric field $E_{x,y}$. Those points (lines), as usual for quantum chain systems, are determined by the dispersion law ε_k. It is easy to see that for $[a_1^2 - a_2^2]E_y^2 < (J - a_3 E_x)^2$ the dispersion law is gapped for all k except of the value of $H = H_{c1} = I$ at which the dispersion law is gapless at $k = 0$. On the other hand, the dispersion law is gapless for $[a_1^2 - a_2^2]E_y^2 \geqslant (J - a_3 E_x)^2$ and $H^2 \leqslant H_{c_2}^2 = I^2 + [a_1^2 - a_2^2]E_y^2 - (J - a_3 E_x)^2$. The critical lines at $H = 0$ as a function of the external electric field are determined from the formula $[a_1^2 - a_2^2]E_{cy}^2 = (J - a_3 E_{cx})^2$.

Let us consider the effect of E_x and E_y separately, starting with the case $E_x \neq 0$ and $E_y = 0$.

Figures 1–3 present the temperature and electric field E_x behavior of the specific heat, electric expansion coefficient, and the electric Grüneisen parameter $\Gamma_{ex} = -\alpha_{exT}/c_V$ for the biaxial spin-1/2 chain (we use $I = 1$, $J = 0.3$, and $a_3 = 1$ for figures below) for $E_y = 0$ and $H = 0$.

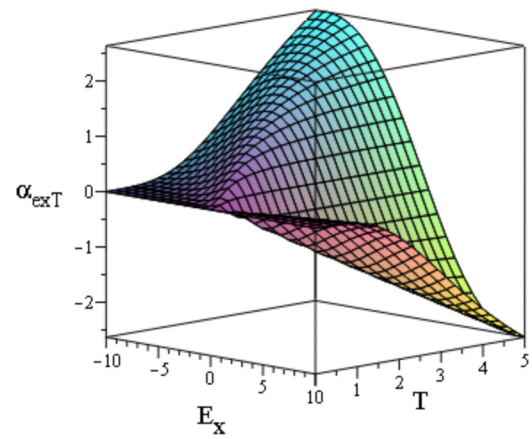

FIG. 2. The electric expansion coefficient of the biaxial spin chain in the absence of external magnetic field as a function of the temperature and the applied external electric field E_x.

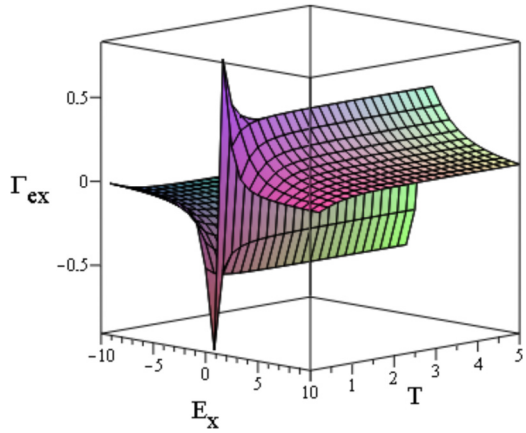

FIG. 3. The electric Grüneisen parameter of the biaxial spin chain in the absence of external magnetic field as a function of the temperature and the applied external electric field E_x.

We can see the changes of the low-temperature behavior of the specific heat and the electric expansion coefficient at $E_x = E_{cx} = J/a_3$. In particular, the specific heat at the critical point changes the low-temperature behavior from the exponential growth with T to the linear one, and the electric expansion coefficient changes sign. However, those changes are relatively small and smooth. Instead, the behavior of the electric Grüneisen parameter clearly shows the features related to the quantum critical point E_{cx}.

Figures 4 and 5 show the behavior of the electric Grüneisen parameter in nonzero magnetic field. In Fig. 4, the case $H = H_{c1} = 1$ is shown. One can see only a quantitative difference between this case and the case $H = 0$ (see Fig. 3): The feature at $E_x = E_{cx}$ becomes larger. In Fig. 5, the behavior of the electric Grüneisen parameter is presented for large magnetic field $H = 3$. We see that the character of the behavior remains similar to the small magnetic field situation; however, the feature at the critical value of the electric field E_{cx} becomes smooth, and the value of the Grüneisen parameter becomes smaller. Notice that the low-temperature specific heat for large values of H grows exponentially with the temperature.

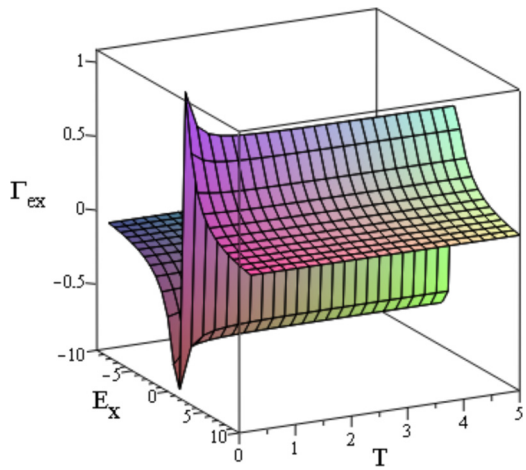

FIG. 4. The electric Grüneisen parameter of the biaxial spin chain in the critical external magnetic field $H = I$ as a function of the temperature and the applied external electric field E_x.

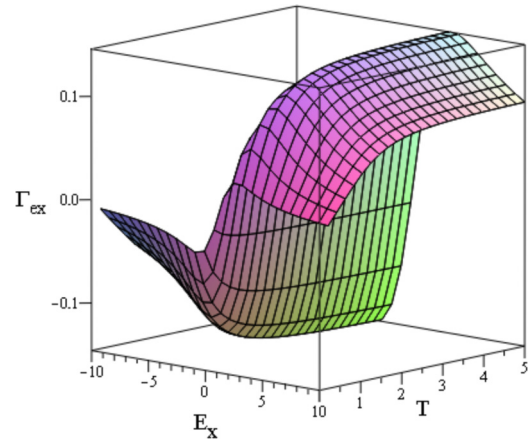

FIG. 5. The electric Grüneisen parameter of the biaxial spin chain in the large external magnetic field $H = 3$ as a function of the temperature and the applied external electric field E_x.

The effect of the z-z spin-spin interaction can be analytically taken into account, e.g., using the Hartree-Fock-like approximation. Consider for simplicity, e.g., the case at which $a_1 = 0$. The Hamiltonian (6) in this case can be rewritten as

$$\begin{aligned}\mathcal{H}_{a_1=0} = &-\frac{N[J_z + 2H]}{4} \\ &- \sum_k \Big[(H - I_1 \cos(k) - J_z) a_k^\dagger a_k \\ &+ \frac{J_1}{2} \sin(k)(a_{-k} a_k + \text{H.c.}) \Big] \\ &+ \frac{J_z}{N} \sum_{k_1+k_2=k_3+k_4} \cos(k_1 - k_4) a_{k_1}^\dagger a_{k_2}^\dagger a_{k_3} a_{k_4}, \end{aligned} \quad (11)$$

where we take I_1 and J_1 at $a_1 = 0$. The parameters [21]

$$\begin{aligned} s &= \langle S_j^z \rangle, \\ r &= 2\langle S_j^x S_{j+1}^x + S_j^y S_{j+1}^y \rangle, \\ q &= 2\langle S_j^x S_{j+1}^x - S_j^y S_{j+1}^y \rangle, \end{aligned} \quad (12)$$

satisfy the self-consistency equations

$$\begin{aligned} s &= \frac{1}{2N} \sum_k \frac{\tilde{A}_k}{\tilde{\epsilon}_k} \tanh\left(\frac{\tilde{\epsilon}_k}{2T}\right), \\ r &= -\frac{1}{N} \sum_k \frac{\tilde{A}_k \cos(k)}{\tilde{\epsilon}_k} \tanh\left(\frac{\tilde{\epsilon}_k}{2T}\right), \\ q &= -\frac{i}{N} \sum_k \frac{\tilde{B}_k \sin(k)}{\tilde{\epsilon}_k} \tanh\left(\frac{\tilde{\epsilon}_k}{2T}\right). \end{aligned} \quad (13)$$

In the Hartree-Fock-like approximation, we use

$$\begin{aligned} \tilde{A}_k &= H + 2sJ_z - (I_1 - rJ_z)\cos(k), \\ \tilde{B}_k &= -i(J_1 + qJ_z)\sin(k), \\ \tilde{\epsilon}_k &= \sqrt{\tilde{A}_k^2 + |\tilde{B}_k|^2}, \end{aligned} \quad (14)$$

where brackets denote the Gibbs distribution with the Hamiltonian $\mathcal{H}_{a_1=0} \approx \sum_k \tilde{\epsilon}_k c_k^\dagger c_k + C$, the fermion operators c_k ($c_k^\dagger$)

are destruction (creation) operators, in which $\mathcal{H}_{a_1=0}$ is diagonal in the Hartree-Fock-like approximation, and C is the operator-independent value. In this approach, the nonzero value of J_z renormalizes the parameters of (8) and, hence, (7). In the ground state, we get

$$s = \frac{1}{2N}\sum_k \frac{\tilde{A}_k}{\tilde{\epsilon}_k},$$
$$r = -\frac{1}{N}\sum_k \frac{\tilde{A}_k \cos(k)}{\tilde{\epsilon}_k},$$
$$q = -\frac{i}{N}\sum_k \frac{\tilde{B}_k \sin(k)}{\tilde{\epsilon}_k}. \tag{15}$$

The right-hand sides of Eqs. (15) in the thermodynamic limit $N \to \infty$ can be written via complete elliptic integrals. The ground-state features (related to the quantum phase transition) of the behavior of the electric Grüneisen parameter exist for $E_y = 0$ at $E_x = (J + qJ_z)/a_3$, at which value the Grüneisen ratio changes its sign. For $E_x = 0$, the feature of the electric Grüneisen parameter can exist for negative q with $(qJ_z)^2 > J^2$ at $E_y = \sqrt{(qJ_z)^2 - J^2})/a_2$. At high temperatures (at which the values s, r, and q are inverse proportional to T, i.e., they are small), the electric Grüneisen parameter for $J_z \neq 0$ taken into account in the Hartree-Fock-like approximation tends to constant at $T \to \infty$.

In the absence of the magnetic field, the behavior of the biaxial spin chain for $a_1 = 0$ is known exactly from the Bethe ansatz solution for $J_z \neq 0$ [25]. Consider the case $E_y = 0$ and $E_x \neq 0$. Let us, by adapting the results of Ref. [26], denote $J_1/I = -k^2\mathrm{sn}^2(i\eta, k)$, and $J_z/I = \mathrm{cn}(i\eta, k)\mathrm{dn}(i\eta, k)$, where we use the Jacobi elliptic sinus, cosine, and delta functions with the elliptic modulus k (do not confuse with the quasimomentum of excitations for the case $J_z = 0$ and the Hartree-Fock like calculations). In such a notation, we can use, e.g., the elliptic modulus as being responsible for nonzero J_1 and the parameter η for the definition of the value of J_z; however, other definitions are also possible [27]. Thermodynamics of the chain is described by the solution of the set of nonlinear integral equations [26]. At high temperatures $T \gg I, J, J_z$, one gets for the free energy $F = -TN\ln 2$, as it must be, so that the entropy in this limit is constant, as for the case $J_z = 0$. The case of low temperatures is more complicated. Consider, for example, the antiferromagnetic interactions. Then the low-temperature free energy of the spin chain can be written as

$$\frac{F}{N} = e_0 - \exp(-e_0/T)[B_1 T^{3/2} + B_2 T^{5/2} + O(T^{7/2})], \tag{16}$$

where

$$B_1 = [iI\mathrm{sn}(i\eta, k)]^{1/2}\left[\frac{K(1-k_1)}{\pi K_1 k_1}\right]^{1/2},$$
$$B_2 = [iI\mathrm{sn}(i\eta, k)]^{3/2}\frac{1-k_1^3}{4\sqrt{\pi}}\left[\frac{K}{K_1 k_1(1-k_1)}\right]^{3/2},$$
$$e_0 = iI\mathrm{sn}(i\eta, k)\left[\frac{K_1}{2K} - k_1\right], \tag{17}$$

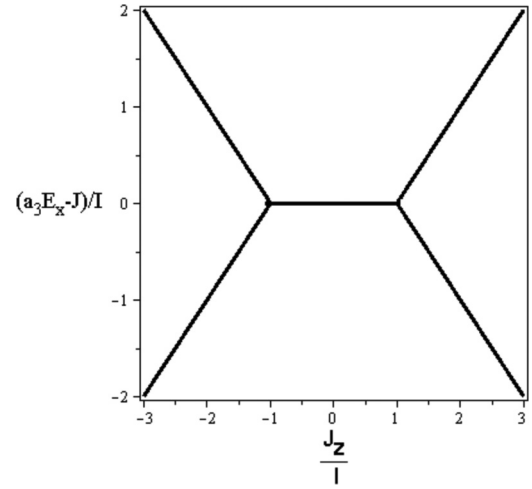

FIG. 6. The quantum critical lines of the spin chain for the general case of exchange parameters $J_{x,y,z}$ in the absence of the external magnetic field as a function of E_x.

where K is quarter period of the elliptic functions, related to k via the parameter q (do not confuse this with the self-consistency parameter of the Hartree-Fock-like calculations)

$$K = \frac{\pi}{2}\prod_{n=1}^{\infty}\left[\frac{1+q^{2n-1}}{1-q^{2n-1}}\frac{1-q^{2n}}{1+q^{2n}}\right]^2,$$
$$k = 4\sqrt{q}\prod_{n=1}^{\infty}\left[\frac{1+q^{2n}}{1+q^{2n-1}}\right]^4 \tag{18}$$

[the conjugated quarter period $K' = \pi^{-1}\ln(q^{-1})$ so that $q = \exp(-\pi K'/K)$], and the additional modulus k_1 defined via the parameter q_1 [with the quarter periods K_1 and K_1' related to q_1 as $q_1 = \exp(-\pi K_1'/K_1)$] is determined from the condition [25]

$$\ln q_1 = -\frac{\pi\eta}{K}. \tag{19}$$

Thus, the low-temperature part of the entropy of the spin chain is exponentially small:

$$\frac{\mathcal{S}}{N} = \exp(-e_0/T)\left(B_1\left[\frac{e_0}{\sqrt{T}} + \frac{3\sqrt{T}}{2}\right]\right.$$
$$\left. + B_2\left[e_0\sqrt{T} + \frac{5T^{3/2}}{2}\right] + \cdots\right). \tag{20}$$

Therefore, the low-temperature specific heat and the electric expansion coefficient are exponentially small.

For the ferromagnetic case, the situation is more complicated; however, the low-temperature part of the free energy of the spin chain also decays exponentially with the temperature [26], except for critical lines (see below).

At the critical lines at which quantum phase transitions take place (e.g., related to the limiting case $k \to 1$ and real η, or $k \to 0$ with imaginary η; see the phase diagram in Fig. 6 below), the low-temperature part of the free energy is

$$\frac{F}{N} = e_0 - \frac{\pi T^2}{6v}, \tag{21}$$

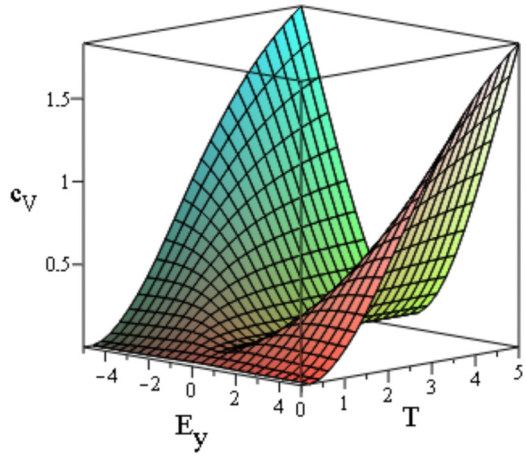

FIG. 7. The specific heat of the biaxial spin chain in the absence of external magnetic field as a function of the temperature and the applied external electric field E_y.

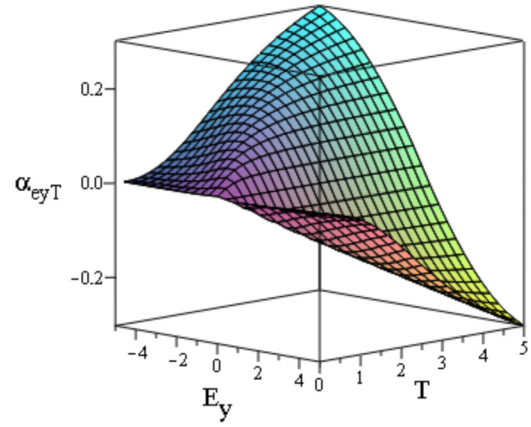

FIG. 8. The electric expansion coefficient of the biaxial spin chain in the absence of external magnetic field as a function of the temperature and the applied external electric field E_y.

with the renormalized ground-state energy e_0 and with v being the velocity of the low-energy gapless excitation (for example, at $k \to 1$ and real η the velocity is equal to $v = (I\pi \sin(2\eta)/2\eta)$, so that the low-temperature entropy is $\mathcal{S} = NT/3v$. The low-temperature specific heat and the electric expansion coefficient are linear in T.

The features of the behavior (in particular, the change of the sign) of the electric Grüneisen parameter Γ_{ex} exist at the quantum critical lines shown in Fig. 6; cf. Ref. [28]. At the quantum critical lines elementary excitations of the system become gapless, while for other values of E_x they are gapped. This situation is similar to the case $J_z = 0$. Therefore, the features in the behavior of the electric Grüneisen parameter for the biaxial spin chain with $J_z \neq 0$ are expected to manifest themselves at low temperatures, similar to the behavior presented in Fig. 3 for $J_z = 0$. At high temperatures, the electric Grüneisen parameter tends to constant for the biaxial spin chain with $J_z \neq 0$, as in the case $J_z = 0$. There are no additional features in the behavior of the electric Grüneisen ratio at intermediate temperatures for the biaxial spin chain with $J_z \neq 0$, similar to the situation with $J_z = 0$.

For instance, for the easy-plane-like case $-I < J_z < I$ at $E_x = J/a_3$, the low-temperature part of the free energy is described by Eq. (21), and the electric Grüneisen parameter manifests peculiarities similar to the case with $J_z = 0$. For any other values of E_x in this easy-plane-like region, the low-temperature part of the free energy is described by Eq. (16), and there are no features in the behavior of the electric Grüneisen parameter. However, for the easy-axis-like case $J_z > I$ or $J_z < -I$, at $E_x = J/a_3$ the low-temperature part of the free energy is described by Eq. (16) or similar for the ferromagnetic case, so that there are no low-temperature peculiarities in the behavior of the electric Grüneisen parameter at $E_x = J/a_3$. Instead, the peculiarities are at the lines $E_x = (J + J_z - I)/a_3$ and $E_x = (J - Jz + I)/a_3$ for $J_z > I$, and at $E_x = (J + J_z + I)/a_3$ and $E_x = (J - J_z - I)/a_3$ for $J_z < -I$; see Fig. 6. At those lines, the low-temperature part of the free energy is described by Eq. (21), while for other values of the the electric field E_x the low-temperature part of the free energy is described by Eq. (16) or similar for the ferromagnetic case.

Let us now turn to the case $E_x = 0$ with $E_y \neq 0$ for $J_z = 0$. This situation is more complicated than previously considered case $E_x \neq 0$ with $E_y = 0$ at which the magnetic anisotropy of the spin system remains orthorhombic (except of the critical values E_{cx}), because the electric field E_y produces monoclinic magnetic anisotropy.

Figures 7–9 manifest the temperature and electric field E_y behavior of the specific heat, electric expansion coefficient, and the electric Grüneisen parameter $\Gamma_{ey} = -\alpha_{eyT}/c_V$ for the biaxial spin-1/2 chain (we use $I = 1$, $J = 0.3$, $a_1 = 1$, and $a_2 = 0.5$ for all figures below) for $E_x = 0$ and $H = 0$.

We see that the temperature and electric field behavior of the specific heat and the electric expansion coefficient is similar to those, obtained for the electric field E_x in the absence of the magnetic field (see Figs. 1 and 2). On the other hand, the electric Grüniesen parameter for this direction of the electric field, which changes sign at the critical value $E_{cy} = J/\sqrt{a_1^2 - a_2^2}$, has different low-temperature behavior compared to the case $E_x \neq 0$ (cf. Fig. 3). In particular, there exists a minimum in the low-temperature dependence of Γ_{ey}, which was absent for Γ_{ex}. That minimum is related to the

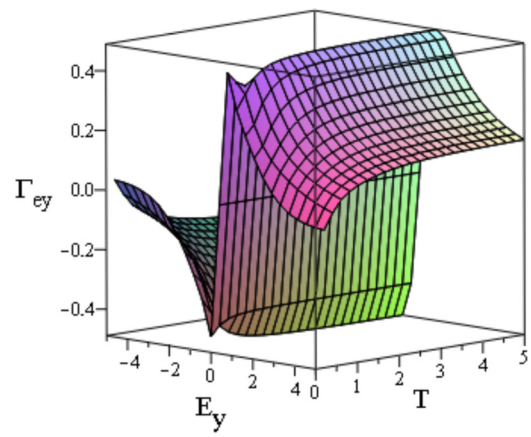

FIG. 9. The electric Grüneisen parameter of the biaxial spin chain in the absence of external magnetic field as a function of the temperature and the applied external electric field E_y.

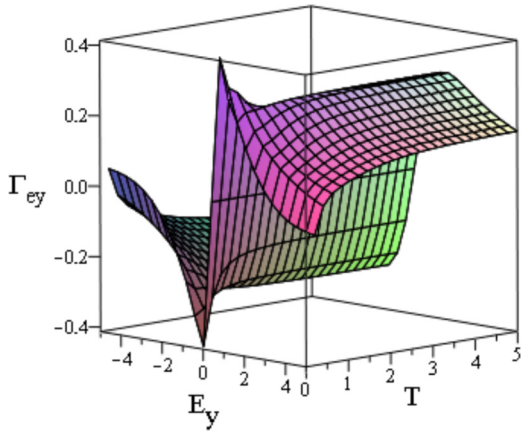

FIG. 10. The electric Grüneisen parameter of the biaxial spin chain for the external magnetic field $H = 1$ as a function of the temperature and the applied external electric field E_y.

features of the spectrum ε_k for $E_y \neq 0$, which are absent for $E_x \neq 0$.

Figure 10 shows the behavior of the electric Grüneisen parameter for the intermediate value of the external magnetic field $H = 1$. For $E_y = E_{cy}$, this point corresponds to $H = H_{c2}$. The behavior of the electric Grüneisen parameter at this tricritical point differs from the one at $H = H_{c1}$ for x direction of the electric field, cf. Fig. 4, and from the behavior at zero magnetic field.

Finally, Figs. 11 and 12 show the temperature and electric field behavior of the specific heat and the electric Grüneisen parameter in the strong magnetic field $H = 3$. Here the strong field H produces the gap in the spectrum of elementary excitations, and hence the low-temperature specific heat increases exponentially with T for all values of E_y (similar to the case with $E_x \neq 0$). The electric Grüneisen parameter, similar to the case $E_x \neq 0$; see Fig. 5) changes sign at $E_y = E_{cy}$; however, there is no feature at that critical value of the electric field. The nonmonotonic low-temperature behavior of the electric

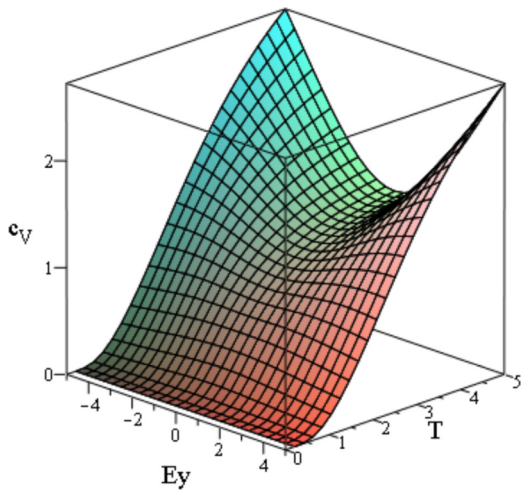

FIG. 11. The specific heat of the biaxial spin chain in the strong external magnetic field $H = 3$ as a function of the temperature and the applied external electric field E_y.

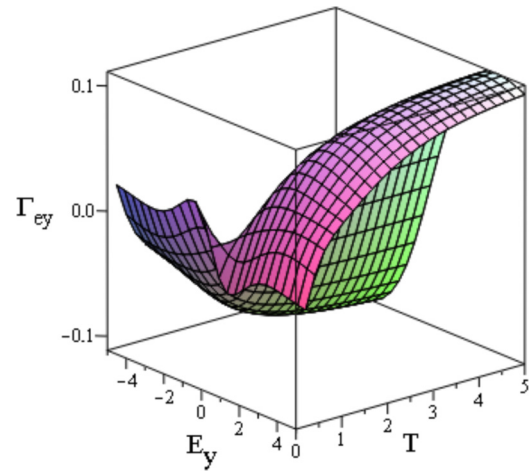

FIG. 12. The electric Grüneisen parameter of the biaxial spin chain for the strong external magnetic field $H = 3$ as a function of the temperature and the applied external electric field E_y.

Grüneisen parameter for the y direction of the electric field (see Figs. 9, 10, and 12), compared to the x direction (see Figs. 3–5) is related to the more complicated ground-state phase diagram in the electric and magnetic field for the $E_y \neq 0$ ($E_x = 0$) case with respect to the $E_x \neq 0$ ($E_y = 0$) one.

Unfortunately, for the monoclinic situation with $a_1 \neq 0$, induced by E_y in the biaxial spin chain, even for $H = 0$ there are no exact solutions for nonzero J_z. However, we suppose that there must exist critical values of the electric field E_y (related to the points of the spectra of elementary excitations, at which the gap is closed), and the electric Grüneisen parameter of the biaxial spin chain with $J_z \neq 0$ will manifest changes of sign and low-temperature features, similar to the case $J_z = 0$, and tends to constant at high temperature.

We are not aware of data of electrocaloric experiments for spin-chain compounds. Our results can be considered as predictions for possible electrocaloric experiments in such systems. It is possible, however, to estimate values of the magnetoelectric coupling constants in real compounds with the magnetoelectric interaction, $a_{1,2,3}$, using, e.g., the results of experiment for the samarium ferroborate [23]. Their values at low temperature were about 7×10^{-2} μC/m^2. The critical values of the electric field are determined by the value of the in-plane magnetic anisotropy J. For spin-chain compounds, the latter is of order of Δg^2 (here Δg is the difference between the effective in-plane g factors) times the isotropic exchange along the chain [20]. For spin-chain compounds, that difference can be on the order of 0.01–0.1 [29,30]. For organic spin-chain systems, the isotropic exchange is of order of 10 K [31], and for spin-chain crystals it can be of order of 100 K [32]. For instance, for the spin-chain crystal 6(MAP)$CuCl_2$ the isotropic exchange parameter along the chain is 110 K, while the in-plane magnetic anisotropy is 0.76 K [32].

V. SUMMARY

In summary, we have studied the quantitative characteristics of the electrocaloric effect in the quantum biaxial spin chain system. We have shown that the introduced electric

Grüneisen parameter demonstrates the critical behavior at the quantum critical points and lines reminiscent to the behavior of similar magnetic Grüneisen parameters for the spin chains. At nonzero low temperatures, the electric Grüneisen ratios shows the change of its sign and strong enhancement at $T \to 0$. Such a behavior is the manifestation of the quantum nature of the low-dimensional many-body spin system. We expect that the predicted behavior can be observed in real biaxial spin chain compounds, because while the coefficients $a_{1,2,3}$ can be relatively small there, the orthorhombic magnetic anisotropy J (which determines the values of the critical electric fields) is also small in typical spin-chain systems, and hence the values of critical electric fields can be accessed in experiments.

ACKNOWLEDGMENT

Support from the DFG via the SFB 1143 is acknowledged.

[1] S. Fähler, U. K. Rössler, O. Kastner, J. Eckert, G. Eggeler, H. Emmerich, P. Entel, S. Müller, E. Quandt, and K. Albe, Adv. Eng. Mater. **14**, 10 (2012).
[2] X. Moya, S. Kar-Narayan, and N. D. Mathur, Nat. Mater. **13**, 439 (2014).
[3] T. Correlia and Q. Zhang, *Electrocaloric Materials: New Generation of Coolers* (Springer, Berlin, 2014).
[4] E. Grüneisen, Ann. Phys. **331**, 211 (1908).
[5] E. Grüneisen, Ann. Phys. **344**, 257 (1912).
[6] L. Zhu, M. Garst, A. Rosch, and Q. Si, Phys. Rev. Lett. **91**, 066404 (2003).
[7] M. Garst and A. Rosch, Phys. Rev. B **72**, 205129 (2005).
[8] M. Gen, T. Nomura, D. I. Gorbunov, S. Yasin, P. T. Cong, C. Dong, Y. Kohama, E. L. Green, J. M. Law, M. S. Henriques, J. Wosnitza, A. A. Zvyagin, V. O. Cheranovskii, R. K. Kremer, and S. Zherlitsyn, Phys. Rev. Res. **1**, 033065 (2019).
[9] R. Küchler, P. Gegenwart, J. Custers, O. Stockert, N. Caroca-Canales, C. Geibel, J. G. Sereni, and F. Steglich, Phys. Rev. Lett. **96**, 256403 (2006).
[10] A. Steppke, R. Küchler, S. Lausberg, E. Lengyel, L. Steinke, R. Borth, T. Lühmann, C. Krellner, M. Nicklas, C. Geibel, F. Steglich, and M. Brando, Science **339**, 933 (2013).
[11] M. Fiebig, J. Phys. D: Appl. Phys. **38**, R123 (2005).
[12] W. Eerenstein, N. D. Mathur, and J. F. Scott, Nature (London) **442**, 759 (2006).
[13] K. Wang, J.-M. Liu, and Z. Ren, Adv. Phys. **58**, 321 (2009).
[14] Y. Tokura, S. Seki, and N. Nagaosa, Rep. Prog. Phys. **77**, 076501 (2014).
[15] S. Dong, J.-M. Liu, S.-W. Cheong, and Z. Ren, Adv. Phys. **64**, 519 (2015).
[16] S. Dong, H. Xiang, and E. Dagotto, Nat. Sci. Rev. **6**, 629 (2019).
[17] U. Adem, L. Wang, D. Fausti, W. Schottenhamel, P. H. M. van Loosdrecht, A. Vasiliev, L. N. Bezmaternykh, B. Büchner, C. Hess, and R. Klingeler, Phys. Rev. B **82**, 064406 (2010).
[18] L. D. Landau and E. M. Lifshitz, *Electrodynamics of Continuous Media* (Pergamon Press, Oxford, UK, 1984).
[19] N. D. Mermin and H. Wagner, Phys. Rev. Lett. **17**, 1133 (1966).
[20] A. A. Zvyagin, *Quantum Theory of One-Dimensional Spin Systems* (Cambridge Scientific, Cambridge, UK, 2010).
[21] A. A. Zvyagin, Phys. Rev. B **103**, 214410 (2021).
[22] A. A. Zvyagin, Phys. Rev. B **105**, 134409 (2022).
[23] T. N. Gaydamak, I. A. Gudim, G. A. Zvyagina, I. V. Bilych, N. G. Burma, K. R. Zhekov, and V. D. Fil, Phys. Rev. B **92**, 214428 (2015).
[24] P. Jordan and E. Wigner, Z. Phys. **47**, 631 (1928).
[25] R. J. Baxter, Phys. Rev. Lett. **26**, 834 (1971).
[26] A. Klümper, Z. Phys. B **91**, 507 (1993).
[27] R. J. Baxter, Ann. Phys. **70**, 323 (1972).
[28] B. Sutherland, J. Math. Phys. **11**, 3183 (1970).
[29] See, e.g., E. Frikkee and J. van den Handel, Physica **28**, 269 (1962).
[30] H. Tanaka, T. Ono, S. Maruyama, S. Teraoka, K. Nagata, H. Ohta, S. Okubo, S. Kimura, T. Kambe, H. Nojiri, and M. Motokawa, J. Phys. Soc. Jpn. **72**, 84 (2003).
[31] H. Kühne, A. A. Zvyagin, M. Günther, A. P. Reyes, P. L. Kuhns, M. M. Turnbull, C. P. Landee, and H.-H. Klauss, Phys. Rev. B **83**, 100407(R) (2011).
[32] M. Ozerov, A. A. Zvyagin, E. Čižmár, J. Wosnitza, R. Feyerherm, F. Xiao, C. P. Landee, and S. A. Zvyagin, Phys. Rev. B **82**, 014416 (2010).